Geotech Geol Eng (2023) 41:1453–1472
https://doi.org/10.1007/s10706-022-02347-8

ORIGINAL PAPER

Alteration Under Wet/Dry Cycles of a Carbonated Clay-Rich Soil from Azazga Landslide Site

Sabrina Haddad · Bachir Melbouci · Fabien Szymkiewicz · Myriam Duc · Ouali Amiri

Received: 20 September 2020 / Accepted: 24 November 2022 / Published online: 6 December 2022

Abstract The weathering of rocks, especially the clay-rich rocks submitted to chemical attack or wet/dry cycles, may impact negatively the slopes stability. This study aims to characterize the alteration of a carbonated clay-rich material assimilated to a marl after the infiltration of polluted water as observed on Azazga site (Algeria) identified as a landslide area. The marl alteration was simulated in laboratory by wet/dry cycles and the level of material degradation was estimated using geotechnical tests (direct shear tests and fragmentation test) as well as physico-chemical measurements and microstructural observations by X-ray diffraction, mercury intrusion porosimetry, chemical analysis and scanning electron microscopy. The effect of wet/dry cycles with artificially polluted water was compared to cycles without pollutants. The tested carbonated clay-rich material composed by around 30.6% of quartz, 12.5% of carbonates and 45.1% of clays showed a higher degradation in contact with polluted water considered as an activator of the degradation. The soil porosity was evaluated with wet /dry cycles and it was estimated from 19.2 to 25% after the cycles. The degradability test (fragmentation test) agreed with the shear test results with a decrease of the cohesion c' from 49.9 to 31.5 kPa (while the friction angle remained close to 20°). Results were confirmed at micro scale with few mineralogical changes and with a higher particle aggregation in presence of pollutants resulting in rough surface while a microporosity around 30 µm appeared after cycles with or without pollutants, probably between disaggregated elongated grains or staked plans observed by SEM. In conclusions, wet/dry cycles with water (without pollutant) were mainly responsible to the disaggregation of carbonated clay-rich soil and pollutants reinforced such effect.

Keywords Marl · Carbonated clay-rich soil · Alteration · Pollution · Laboratory tests · Landslide

S. Haddad (✉) · B. Melbouci
Laboratoire Géomatériaux Environnement et Aménagement, Université Mouloud Mammeri, 15000 Tizi-Ouzou, Algérie
e-mail: sabrinahaddad0617@gmail.com

F. Szymkiewicz · M. Duc
Université Gustave Eiffel, GERS/SRO, 5 boulevard Newton, Champs-sur-Marne, 77454 Marne-la-Vallée, France

O. Amiri
GeM, Ecole d'ingénieurs de l'Université de Nantes, boulevard de l'Université CS 70152, 44603 Saint-Nazaire, France

1 Introduction

Various weathering processes occur in carbonated clay-rich soil such as physico-chemical phenomena: cracking under freeze-thaw cycles or thermal variation, change of porosity under dissolution, mineralogical transformation under gas or water. Such

processes usually decrease the mechanical strength of the material (Cafaro and Cotecchia 2001; Li et al. 2018; Ogunsola et al. 2017; Saad et al. 2010; Serratrice 2017; Sousa et al. 2005). So, the stability of the soil especially in landslide area and the risk of rupture caused by the material alteration depend on the degradation kinetic as well as the initial characteristics of soils (friction angle, cohesion, density, etc.), the soil water content (degree of saturation, suction or pore pressure), the slope angle and the vegetation cover. Both climate change (rains) and anthropic activities (water infiltration or pumping) can also impact the site characteristics and then affect the slope stability (Li et al. 2018; Viville et al. 2012). The water circulations in soil mainly govern the rate of material weathering (Hausrath et al. 2011; Lofi et al. 2012) and represent a major factor that triggers the ground movements (Aurelie 2010; Gabet et al. 2010; Pomerol et al. 2005). This is particularly true in clay-rich soils characterized by a variable shear strength that depends on the soil mineralogy, its microstructure (density, porosity) and the soil water content. According to Guigo (1979), the montmorillonite-rich or illite-rich soils are able to retain great quantities of water, changing their rheological state from solid to liquid state. Such soils are known to be able to experience mass movements causing strong slope dynamic, especially in presence of high water content.

At microscale, the soil porosity plays a major role in the chemical weathering by allowing the penetration of harmful species. The size, morphology, connectivity and the distribution of voids inside soils (or rocks) depend on the matrix compactness and the particles/minerals arrangement. Such parameters govern the water permeability (Emmanuel et al. 2015; Ogunsola et al. 2017; Tindall 1999; Tugrul 2004; Quénée 1990). The pores size proves to be a more important parameter than the total pore volume according to Iniguez Herrero (1967). As stated by Mamillan and Bouineau (1982), materials with a high content of fine pores appear as less resistant to weathering because capillary phenomenon may occur, while materials with higher 20% of porosity show usually the strongest mineralogical evolution according to Quénée (1990). Climatic, biological and mechanical factors may also contribute to increase the pore dimension by dissolution or their decrease by precipitation or filling after clay or fine particles transport during erosion process (Goodfellow et al. 2016). Change of compactness by mechanical alteration under swelling/shrinkage cycles in presence of water (Hamès et al. 1987) or after freezing/thawing cycles or burst phenomenon, impact also the pore structure as well as the salt crystallization in confined pore space (Goodfellow et al. 2016; Labus and Bochen 2012; Tindall 1999). The long term chemical alteration by mineral hydrolysis, oxidation (notably iron-rich minerals and sulphur such as pyrite), by hydration or decarbonation modifies not only the porosity but also the soil mineralogy (Labus and Bochen 2012). In rocks, alteration impacts above all the surface of discontinuities as well as the bridging cementation between grains (Li et al. 2018) while in soil considered as particles arrangement with low cementation and most often a higher porosity compared to a rock porosity, the alteration may concern the whole volume of the material. The dissociation of chemical bonds between minerals and ions (Clark and small 1982) accompanies the mechanical alteration and takes advantage of the soil or rocks cracking and their widening, to progressively reach the whole minerals.

Among rocks, marls are considered as soft rocks, composed mainly by quartz, carbonates and clays. The term marl concern usually material with a carbonate content between 30 and 75%. At lower concentration, the term carbonated clay-rich soil will be preferred. These carbonated materials may dissolve in contact with acidic water but also be submitted to erosion (particles pullout) as in a soil. Studies on Callovo-Oxfordian "Terres Noires" in France put in evidence a clear link between the carbonate content, the clay content (and its swelling potential) with the rate of the material disaggregation (Bufalo et al. 1989; Chodzko and Lecompe 1992; Colas and Dumolard 1988; Monnet et al. 2012). Depending on climate (Aurelie 2010), the temperature and the percolation kinetic, alteration depends also on the water pH and composition (Burnol et al. 2006; Boukoffa 2018). Indeed, groundwaters are increasingly subjected to voluntary or accidental spills of polluted effluents, wastewater from discharges or landfills or chronic contamination from rainwater runoff in urban areas that concentrate air pollutants, leakage from pipes or buried sewerage systems and road leaching (Bower 2002; Pitt et al. 1999). Rainwaters (containing salt especially in coastal area) are often mixed with wastewater from sewerage systems, and they bring chemical elements, which are source of alteration (Fifi et al.

2009). Therefore, the presence of pollutants in water usually impacts the soil properties especially the soil porosity and may accelerate its erosion or alteration (Molina Ballesteros et al. 2010; Wells et al. 2006). Not only the intrinsic properties of pollutants (solubility, adsorption, degradability) impact the pollutant migration, but also the environment properties (permeability, organic matter content, oxidation degree…) (Collin and Collin 2003). Indeed, physical (i.e. temperature), chemical (i.e. oxidation reaction) and biological (i.e. bacterial development) phenomena control the pollutant migration in porous soil (Burnol et al. 2006; Melki et al. 2019; Mulliss et al. 1997).

The mineralogical transformations during alteration operate with the release or the adsorption of elements (Campy and Macaire 2003; Zhang et al. 2009), as during the dissolution of carbonated clay-rich soil where carbonates release for example calcium or magnesium in pore water. Such release interacts strongly with clays especially by ions exchange process (Hounsounou et al. 2016). Carbonated neoformation may also precipitate, entrapping chemical element such as heavy metals.

Many researchers such as (Chen and Ng 2013; Duc et al. 2014; Goh et al. 2014; Pires et al. 2008; Tran 2014), have contributed to the understanding of volumetric deformation and mechanical characteristics of soil during wet-dry cycles through odometer, triaxial, and direct shear tests. Indeed, they concluded that the hydromechanical behaviour of the soils was significantly influenced by the history of the wetting–drying cycles. Effectively, the differences between the shear strength on the drying and wetting cycles of the first cycle were found to be greater than that of the next cycles. They also showed that wet–dry cycles could lead to a rearrangement of the soil particles, a modification of the pore system and also induce soil aggregation. Tisdall et al. (1978) showed that the stability of wetted aggregates decreased with increasing wet–dry cycles.

Many studies on clayey soils focused on deformations caused by climate variations between hot and cold season simulated by cyclic water solicitation (Duc et al. 2014; Geremew et al. 2009; Medjnoun an Bahar 2016; Tripathy et al. 2002). If cycles usually consist in partial drying except in the upper part of in situ soil, most of wet/dry cycles applied in laboratories with complete drying and wetting by immersion imposes strong deformation and strong water gradient, causing various cracking patterns according to the drying kinetic and soil mineralogy. Cycle impact was mainly governed by the amplitude of the humidity change. Marly and clayey soils behaviour differ with the presence of carbonates which are at the origin of a cemented microstructure. If clayey soils develop their whole swelling potential as soon as the first cycles, marls usually show a slow evolution (delayed impact of wet dry cycle) until the total breaking of the cementation.

Finally, leaching/precipitation, erosion (particle displacement with water flow), clogging or swelling change the pore structure in soil and its permeability as well as the soil mechanical strength or the pore pressure balance, which in turn can become unfavourable to slopes stability.

In this paper, a carbonated clay-rich soil from Azazga city in Tizi-ouzou region in Algeria was studied. The city is located at the top of a slope where a major landslide occurred in the past causing significant damages. The rock massif at 20 m was composed by remoulded marl with various carbonates content (mainly calcite and dolomite) laying on a undisturbed marly layer, and in which the circulation of polluted and unpolluted water was suspected to be at the origin of physical and mechanical degradation on both the superficial and deep layers. The polluted waters come from unconnected sewerage network of Azazga city. Wastewaters may either run off down the slope causing erosion before their collect in ravines downstream or infiltrate in fractured soil and rock massif, which promotes the reactivation and progression of the landslide phenomenon. In both case, wastewaters contain chemical agents that may significantly contribute to erosion by soil particles dispersion or to alteration by chemical dissolution and/or precipitation processes. Such phenomenon was identified as a possible threat for the slope stability, which explains the subject of this study.

The present work aims to characterize the weathering phenomenon of a marly material sampled at 20–24 m depth (and designated in this paper with the term soil) under accelerated aging in the laboratory by applying wet/dry cycles with polluted or unpolluted water. Cycles want to simulate the climate conditions in Azazga region in Algeria, where landslide occurred. Experimental tests put in evidence the role of pollutants in water and if such chemical elements

promote or not the soil degradation. After a geological description of landslide site and its geology, the mineralogical and geotechnical characteristics of studied carbonated clay-rich soil were presented. Then, the soil degradation under wet-dry cycles with polluted or unpolluted water was observed at macro (at millimetre scale) and microscale (at micrometer to nanometer scale) using X-ray diffraction, mercury intrusion porosimetry (MIP), scanning electron microscopy (SEM), parallel to direct shear test as well as degradability test measuring the crushing rate of soil. All the results are discussed to conclude on the potential role of pollutants as landslide activator in a carbonated clay-rich soil.

2 Materials and Methods

2.1 The Landslide Site Characterization

Azazga city is located at 20 km east of Tizi-Ouzou in Algeria, at altitudes of about 450 m above the sea level. In this region, a landslide occurred on a 10° to 15° natural slope. According to Ameur (2014) and Djerbal et al. (2014) who provided a historical overview of Azazga landslide movements, the area experienced several ground instabilities since 1952. In last years, the long rainy period in 1974 and the long snowy period in 2012 were followed by strong reactivations of the ground movement and the appearance of major disorders on construction (Fig. 1).

The main factors proposed to explain such phenomenon are related to the hydro-climatic characteristics of the region and the geomorphological nature of the site as well as human activities.

A geological study based on geotechnical reports and the geological map of Azazga landslide area (Fig. 2) distinguished Cretaceous facies (flysch) in most of the region (LCTP 2004).

This formation was partially masked in west by Miocene facies and overlapped in east by Numidian facies. Also present, the red and green sub-Numidian clays with decimetric sandstone banks from Oligocene outcropped east and north-east of Azazga region. Parallel, the Numidian sandstones constituted the main reliefs of the Djebel Abed at eastern end of the region. Furthermore, some massive layers cut into panels by a system of faults, were visible in east of the city. These panels collapsed and Numidian screes composed by sandstone blocks with various sizes coming from the relief of the Djebel Abed, formed land of screes in the centre, north-eastern and south-eastern of Azazga region. All the formations were characterized as allochthon (except screes) that is to say the materials have been moved from their original site of formation. They were displaced during or after their sedimentation and formed two tectonic units: the Azazga flysch unit composed of clay/marl-rich formations with small sandstone layers, and the Numidian unit consisting of Oligoceneous clays at the bottom and Aquitanian sandstone at the summit.

In addition, a complex hydrology characterized the Azazga region, with the presence of a water table close to the surface, the presence of springs downstream of the slope accompanied by several watercourses and areas of stagnant polluted water. Laboratory tests showed that the saturation degree

Fig. 1 Various damages caused by landslide in Azazga region on a **a** sewerage system in March 2012, **b** a house in March 2014, **c** a road with the appearance of subsidence in January 2019

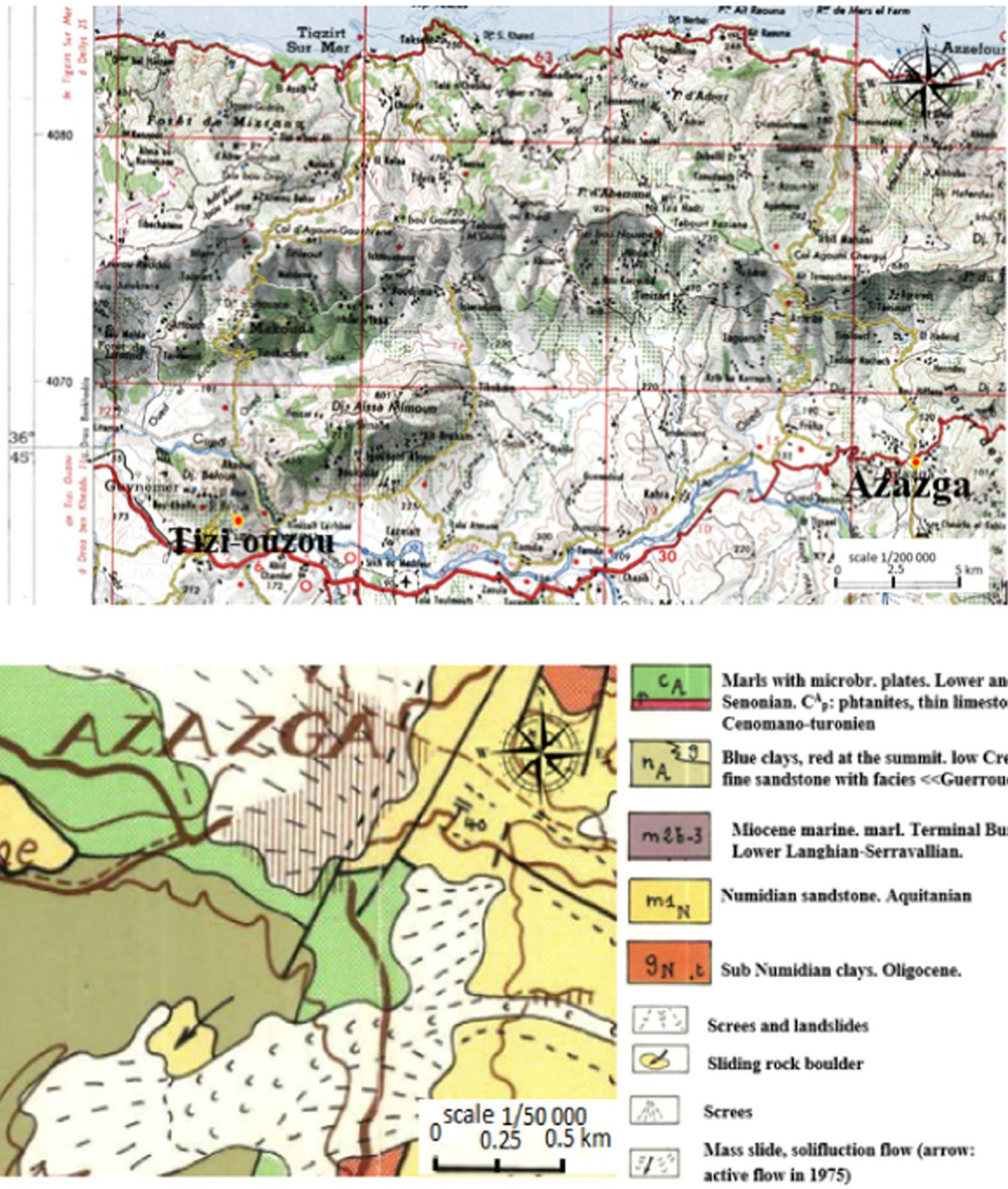

Fig. 2 Location and geological map of Azazga site (Gélard 1979)

of soils sampled near the surface was close to 100%. In addition to this complex hydrology, intense rainfall affected the soil hydrology and contributed to the amplification of the gravitational ground movement despite the gentle slope characterizing the Azazga landslide.

Soil erosion due to the circulation of polluted or unpolluted water and the transport of fine particles into the massif was also detected. The phenomenon is responsible to the usual presence of fine particles after heavy rainfall in spring waters.

Finally, land movements and anthropic activities such as constructions significantly reshaped the slope in landslide area near Azazga (Djerbal et al. 2014) which induced a negative impact on the slope stability. The lack of sewerage and drainage systems in this

area, the deviation of natural watercourses and the clogging of springs, the deforestation in recent years as well as the buildings of construction on unstable ground (which represented an overloading for the slope) were judged as harmful factors for the slope stability.

2.2 Geotechnical Characterization of Site Materials

After a geological and geotechnical investigation (LCTP 2004) to identify soils and estimate the depth and the shape of the landslide surface, boreholes were carried out on Azazga site. They showed the presence of six soil layers. Starting from the surface, a sandy silts layer was followed by a fine sand layer, a friable marly clay, a highly remoulded grey clay, a compact marly clay and the substratum composed by sandstone blocks. The soil layers had an unfavourable dip oriented in the direction of the slope, which favoured the ground movements. The Table 1 gives the geotechnical characteristics of the different Azazga soil layers (LCTP 2004).

The materials observed at the interface between remoulded clay and compact marly clay on Fig. 3 showed a pronounced alteration with a great disturbance. The disturbed clay layer met at about 20 m depth presented fractures that could be mobilized in ground movements. The presence of remoulded zones located at the interface between the substratum and surface layers (LCTP 2003, 2004; LTPC 1987) was identified as weak zone. Such layer, probably remoulded due to the ground movement, was of first importance but it was however unusable for laboratory tests. In order to confirm the soil disturbance by climate wet/dry cycles and its role on the occurrence of remoulded area, samples were taken in three neighbouring cored samplings especially in compact marly clay layer.

Fig. 3 Box showing the soil cores extracted between 21 m deep (first layer of the box) to 24 m deep (bottom layer of the box)

2.3 Experimental Methods

The aim of the experimental program was to study the influence of pollutants in water used to perform wet/dry cycles to alter Azazga carbonated clay-rich soil. These accelerated aging cycles were based on annual temperature and precipitation data recorded on site. Artificial polluted water was prepared to reach similar chemical properties as the polluted water collected at the bottom of the Azazga slope (ONA 2016). Concentrated polluted water contained 20 mg/L of phosphates, 40 mg/L of sulphates and 60 g/L of laundry detergents (bleaching water, shampooing, soap, floor wash). The low concentration of the applied solution (noted LC solution) was composed of 10% of concentrated polluted water, the medium one (MC) of 20%, and the high concentration (HC) of 30%. All the tests were applied on soil submitted to LC water and it was mentioned if HC or MC waters were applied in place of LC water.

The carbonated clay-rich soil samples were subjected to a series of six cycles. Each cycle included a drying step in oven at 45 °C for 16 h and a humidification step by immersion at 5 °C for 8 h. The conditions of the cycles were chosen close to the environmental extreme conditions (Fig. 4) under which the material can be submitted in term of temperature at surface and the short duration of each impacting step was compatible with the working hours (1 day for immersion and one nigh for drying). Under such cycles, the degradation is supposed maximum with strong water gradient in specimens.

After cycles, X-ray diffraction (XRD) analyses were performed on both intact and altered soil samples. Freeze-dried samples were crushed and grinded to pass an 80 µm sieve. XRD patterns were obtained by using a D8 advance diffractometer from Bruker (Cobalt anode, E = 35 kV, I = 40mA, no monochromator, LynxEye detector). A continuous scan mode, between 3 and 80° 2theta, with a rate of 1 s per 0.01° 2theta was selected. Diffractograms were exploited

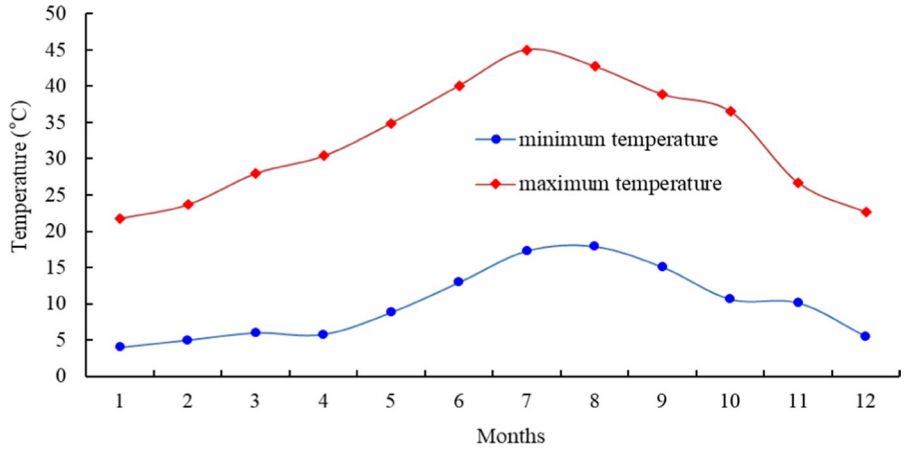

Fig. 4 Minimum and maximum temperature between 2008 and 2017 in Azazga (ONM 2016)

with EVA program coupled with ICPdf2 mineralogical database. Quantitative mineralogy was done using Rietveld method (Topas software).

After cycles, environmental scanning electron microscope (Quanta 400 SEM from FEI) coupled with energy dispersive X-ray spectrometry (EDX from EDAX) allowed to observe the microstructure of marly soil and to estimate the sample degradation at microscale. The chemical composition in both intact and altered soil was estimated with EDX probe which gave an order of magnitude of the chemical content. SEM images were collected on fresh fractured surface on air dried sample and back scattered electron mode was selected in low vacuum mode (no metal coating was applied before analysis).

In parallel, the mercury intrusion porosimetry (MIP) tests were carried out on freeze-dried samples before or after alteration by wet/dry cycles. They completed the SEM observations by quantifying the pore modification under wet/dry cycles. The applied pressure on mercury to intrude into pores ranged from 3.4 kPa at low-pressure up to 230 MPa in high pressure. Therefore, the corresponding pore diameter varied from 6 nm to 355 µm. The porosity lower than 6 nm could not be reached by MIP so the measured total porosity was usually underestimated compared to the water porosity.

At macroscale (millimeter to pluri-millimeter scale), a degradability test (or fragmentation test) was carried out in accordance with the French standard NF P 94-067 (AFNOR 1992). After crushing, two kilograms of 10/20 mm granular intact marly soil were submitted to four cycles of imbibition, either with distilled water or with polluted water for 8 h, followed by a drying in oven for 16 h at 105 ° C. The particle size of the sample was measured by sieving before and after test.

Table 1 Geotechnical characteristics of soils from Azazga site (LCTP 2004)

Soil layer	γ_d (kN/m^3)	γ_h (kN/m^3)	LL	PI
Sandy silt	15.3	19.0	28.6	14.9
Fine sand	14.3	18.5	71.5	32.9
Friable marly clay	17.2	20.1	75.5	37.7
Remoulded clay (colluvion)	15.2	19.2	71.0	32.0
Compact marly clay	*18.3*	*20.1*	*51.0*	*26.2*
Sandstone blocks	19.0	20.1	–	–

In italics, the layer where tested samples in this study were taken

Finally, direct shear tests were carried out, each on at least three cylindrical soil specimens submitted to three different vertical stresses. Each test specimen was cut manually in the core of a bored soil sampling (test was performed on intact soil whose density and water content were given in Table 1). These test specimens underwent until six wet/dry cycles, either in distilled water or in polluted water. Each cycle involved a drying at 45 °C for 16 h and a wetting by immersion at 5 °C for 8 h. After cycles, the test pieces were subjected to direct shear tests at the same speed (in drained consolidated conditions), under 100, 300 or 400 kPa normal stresses.

3 Results

3.1 Properties of Intact Carbonated Clay-Rich Soil from Azazga

Table 2 shows the geotechnical characteristics of intact carbonated clay-rich soil (before wet/dry cycles). Atterberg limits were measured using NF P 94-051 standard (AFNOR 1993) and the soil was classified as very plastic clay (At) according to the USCS-LCPC classification. The dry unit weight of intact soil was $\gamma_d = 18.5$ kN/m^3 and the corresponding void ratio e was equal to 0.43 while the porosity n was estimated to be 30%.

The mineralogical identification of clays in Azazga marly soil was performed on X-ray diffraction pattern obtained on oriented glass slides on Fig. 5 while the XRD powder pattern gave the soil minerals contents in Table 3. Results showed a predominance of clay minerals with the presence of montmorillonite (13.6), kaolinite (14.5%), illite (9.3%) and chlorite (7.7%) as well as quartz (30.6%). The total clay content represented 45.1% of the whole minerals. The XRD analyses on oriented glass slides prepared with the fraction lower than 2 µm extracted from the decarbonated and Na-homoionised soil, confirmed on Fig. 5 the presence of kaolinite (with a peak at d = 7.07 Å that disappeared after heating at 550 °C), the presence of chlorite (with a remaining peak at d = 7.16 Å after heating at 550 °C and a peak at 14.1 Å whatever the glass slide treatment) and the presence of illite (with an invariant peak at d = 9.97 Å).

The large peak at d = 11.97 Å on air-dried glass slide on Fig. 5 shifted toward higher d value close to d = 17 Å after contact with ethylene glycol. After burning at 550 °C, the initial peak at d = 12 Å disappeared and was correlated to the appearance of a peak slightly lower than d = 10 Å. Such behaviour confirmed the presence of swelling smectitic clay such as montmorillonite according to Brindley (1980).

Feldspars (albite and microcline) were also present in low quantities in marly soil, while carbonates (dolomite and calcite) represented around 12.5%. Such phases are able to dissolve in presence of acidic water, which would induce a change in porosity and a lack of cohesion. Indeed, the carbonates play often the role of cement in marly soils. However, this rigid skeleton may be broken gradually by soil swelling/shrinkage. Pyrite was also present in soil as well as gypsum in trace quantity. Gypsum can be formed by precipitation in salted soil but its origin here is more probably link to the oxidation of pyrite FeS_2 in

Table 2 Geotechnical properties of the tested carbonated clay-rich soil as sampled on Azazga site

Characteristics	γ_d (kN/m^3)	γ_h (kN/m^3)	LL	PL	PI	Porosity n	Void ratio e	W (%)
Value	18,5	19,8 (unsaturated)	51	21	30	30%	0,43	33

Table 3 Mineralogical composition of Azazga intact marly soil. For such quantification, the Rwp was equal to 6.06

Rwp is a goodness of Rietveld fit that must be the closest to zero

*The sum of the quantities associated to crystalline phases is equal to 100% and the degree of crystallinity estimated to 76.6% was not considered in such calculation

Minerals	Formula	Mineral family	Quantity (%)*
Quartz	SiO_2	Silicate	30.6
Calcite	$CaCO_3$	Carbonates	8.4
Dolomite	$CaMg(CO_3)_2$	Carbonates	4.0
Montmorillonite	$(Na,Ca)_{0,3}(Al,Mg)_2Si_4O_{10}(OH)_2$	Clay	13.6
Chlorite	$(Fe,Mg,Al)_6(Si,Al)_4O_{10}(OH)_8$	Clay	7.7
Illite	$(Al,Mg,Fe)_2(Si,Al)_4O_{10}(K,H_3O)$	Clay	9.3
Kaolinite	$Al_2Si_2O_5(OH)_4$	Clay	14.5
Albite	$NaAlSi_3O_8$	Feldspars	6.5
Microcline	$KAlSi_3O_8$	Feldspars	1.8
Pyrite	FeS_2	Sulfur	0.4
Gypsum	$CaSO_4.\ 2H_2O$	Sulfate	0.4
Anatase	TiO_2	Oxyde	2.8

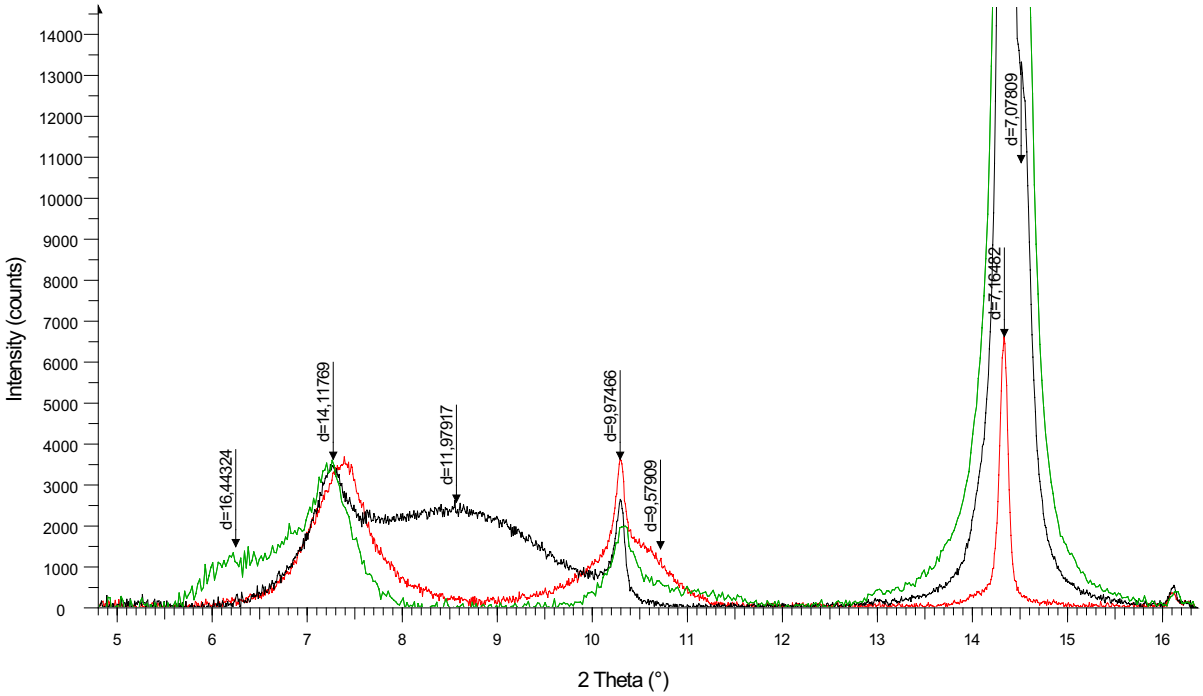

Fig. 5 XRD pattern on oriented glass slides manufactured with the < 2 µm fraction extracted from marly soil. Pattern on air dried oriented glass in black, on oriented glass slide put in contact with ethylene glycol under vapour form (at 55 °C during a night) in green and on oriented glass slide heated at 550 °C in red

contact with oxygen. The sulfuric acid produced by pyrite oxidation reacts with carbonates to form finally gypsum.

According to Guilloux et al. (2005), both mineralogy and porosity allows the classification of argillaceous soil in terms of hardened soils or soft rocks. With a 30% porosity and a clay percentage lower than 50%, the Azazga marly soil was classified at the limit between soils and soft rocks.

Azazga's carbonated clay-rich soil was characterized by a low level of swelling clays and the percentage of carbonates was around 12.5%. Such percentage could help to estimate the weathering rate of such soil. Indeed, Guilloux et al. (2005) proposed that marls with a carbonate content less than 10–20% associated with a significant clay fraction (at least 30%) could be sensitive to water variation with a strong impact of water imbibition that induces swelling in most of case. Indeed, the clay particles in great quantity were able to coat or wrap the fine carbonated particles, which reduced the number of carbonate-carbonate bonds and favoured the soil disaggregation in presence of water. In addition, the non negligible soil porosity around 30% promoted the water circulation in material and contributed also to reduce the soil mechanical resistance.

3.2 Effect of Wet/Dry Cycles with Polluted Water on Soil Mineralogy and Soil Chemical Composition

X-ray diffraction analyses on Fig. 6 was carried out on marly soil before and after 3 or 6 wet/dry cycles with polluted water. Patterns were normalized by using quartz peak at d = 3.34 Å considered as invariant peak (non reactive phase). Normalization consisted to multiply the intensity of each pattern, to reach the same height on the main peak of quartz at d = 3.34 Å. In this case, the other peak can be compared visually from a pattern to another.

As the polluted water composition was fixed at 20 mg/L of phosphates, 40 mg/L of sulphates and 60 g/L of laundry detergents, new precipitated phases were searched on patterns as well as the disappearance of initial phases. A gypsum precipitation with a peak at d = 7.61 Å occurred clearly after wet /dry cycles while the soil before cycles contained only a

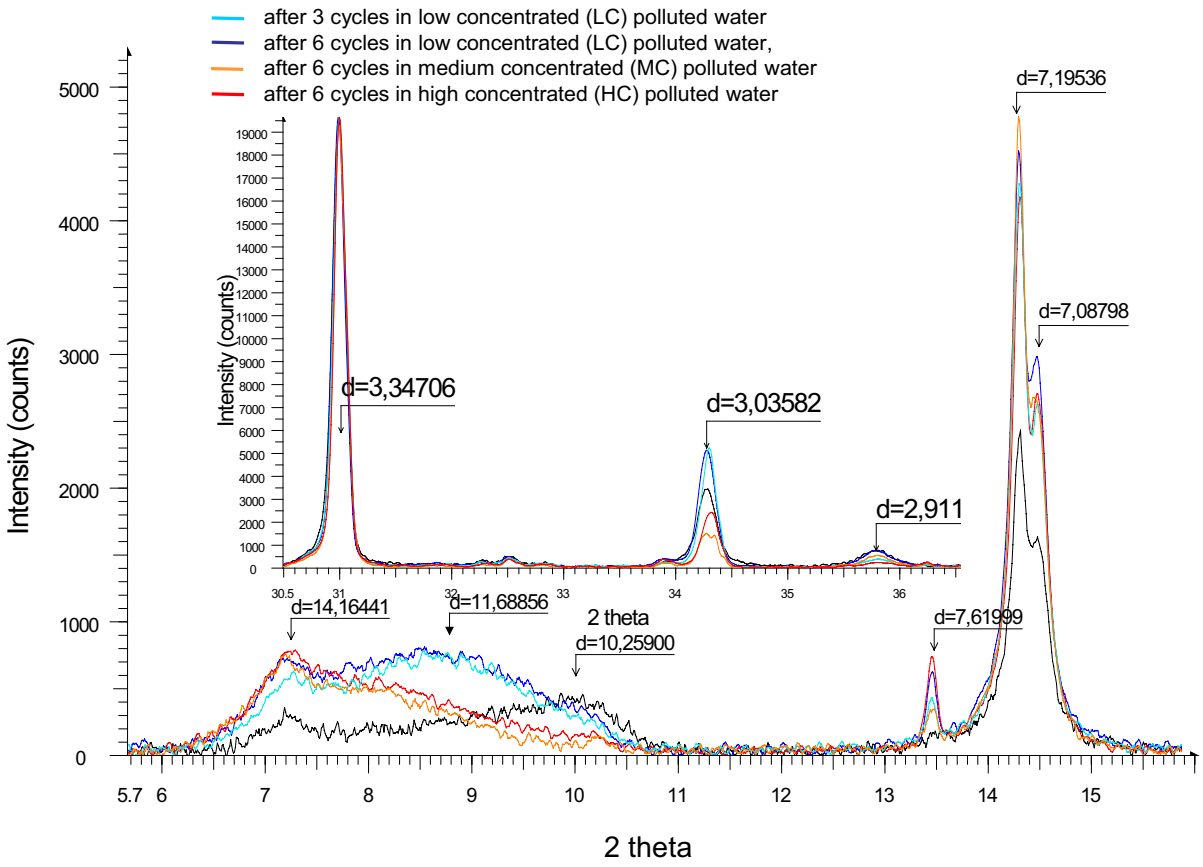

Fig. 6 XRD powder patterns on marly soil before and after wet/dry cycles with polluted water. Patterns were normalized based on quartz peak (at d = 3.34 Å) and corrected by the background subtraction

0.4–0.5% of gypsum/pyrite as shown in Table 3. The gypsum increase may be related to the natural heterogeneity of tested soil but more probably to a precipitation during the air drying of soil, whose pore water contained dissolved calcium and sulphates coming from the polluted water. No other new phases were observed.

At the same time, the intensity of the main XRD peak associated to calcite (d = 3.03 Å) changed after contact with polluted water. As the concentration of polluted water increased (for the red curve on Fig. 6), the peak of calcite decreased gradually because of an enhanced dissolution of carbonates phase in contact with polluted water. The dolomite behaviour (peak at d = 2.91 Å) is not so clear considering the lower intensity of the peak, the possible variability of carbonate content from one tested sample to another, as well as the lower solubility of dolomite in acidic medium (dolomite dissolution required usually higher temperature to occur compared to calcite dissolution).

Furthermore, the shape of the clay peaks between 6 and 11° 2θ seemed to be also impacted after cycles. The chlorite peak at d = 14.16 Å as well as the kaolinite peak at d = 7.08 Å and the large peak associated to montmorillonite evolved. The higher intensity of peaks could be interpreted as a change of clay quantity (because of heterogeneity between tested samples) but also to the level of clay sheet orientation in XRD sample holder. Indeed, the clay disorganization during the wetting during cycles could be followed by more oriented clay particles during the drying that acts as a compaction step. A higher orientation of clay particles may increase the peak height with similar clay content (especially for kaolinite, chlorite and montmorillonite but not for illite).

To better see the effect of the pollutants, patterns were collected on marly soil after 6 wet/dry cycles in contact with medium (MC with 20% of pollutants) and highly (HC with 30% of pollutants) concentrated polluted waters compared to the low (LC with 10% of pollutants) concentrated water used in other tests. In this case the peak attributed to illite at d = 10.25 Å seemed to decrease. Such change was not clearly explained by illite dissolution. Indeed, the pollution in water was not enough concentrated to dissolve efficiently aluminosilicates but a change of clay sheet staking (by dispersion or disorganization) could be at the origin of the peak change. Furthermore, the main change appeared on the peak associated to montmorillonite that shifted from d = 11.7 Å towards higher d value. Considering that XRD patterns were obtained at the same ambient relative humidity in air, the increase of montmorillonite interlayer could be interpreted by cations exchange. Indeed, a sodic montmorillonite interlayer was around 12 Å compared to a calcic one at 14 Å. The nature of cations in interlayer and their ability to adsorb water as well as the relative humidity governed the d spacing of montmorillonite.

After wet/dry cycles, the change in chemical composition of marly soil was also searched by using ICP/OES analysis applied on intact soil and on soil after 3 or 6 cycles with polluted water. Major elements in Table 4 were quantified but no major change was observed.

The total percentage in Table 4 corresponds to the sum of the chemical quantities measured by ICP/OES added to the loss of ignition (LOI) obtained by sample calcination at 1000 °C (the loss of mass after heating corresponds to a water and CO_2 loss). A total value close to 100% indicated that no major elements were forgotten and that the sulphur S content should be low (less than 1%). Such composition agreed with the low quantities of gypsum/pyrite detected by XRD. However, a few other elements or trace elements under the detection limit of ICP/OES or not detected by such technique could be present in the samples. For example, EDX measurements coupled with SEM observations revealed the presence of a 0.3–0.5% chloride content in samples after cycles.

The calcium content slightly increased in Table 4 after 6 wet/dry cycles, which could explain the change of montmorillonite peak on XRD patterns on Fig. 6. At the same time, the quantity of silicium decreased. The calcium released by carbonates dissolution observed by XRD remained in the soil pore water even after immersion and added calcium was probably brought by contact between soil and polluted water. Concerning the Si content, the dissolution of a silicate mineral probably occurred in contact with polluted water. As the degree of crystallinity of initial soil revealed the presence of around 23–24% of amorphous phase in intact marly soil, the dissolution of amorphous silica is proposed to explain the Si increase. However, all these small changes could also be explained by a natural variation of carbonates or silicates between the tested soil specimens. A mineralogical heterogeneity among the cored soil specimens at decimetre to meter scale could not be excluded.

Furthermore, even after 6 cycles composed by 6 immersions in polluted water containing 20 mg/L of phosphates, 40 mg/L of sulphates and 60 g/L of laundry detergents, the P concentration remained quite stable around 0.31–0.33%. No precipitated compound was formed with such element and adsorption on soil mineral surface did not occur. The non affinity of clay towards anionic species could explain such results. Indeed, clays are usually characterized by a permanent negative charge and phosphorus was on negatively charged form (PO_4^{2-}/HPO_4^-) or neutral form (H_2PO_4) according to the pH of the solution (as well as sulphates that could be on SO_4^{2-}/HSO_4^-/H_2SO_4 forms). The conditions were not in favour to pollutant

Table 4 Chemical composition of marly soil before and after wet/dry cycles with polluted water (analysis by ICP/OES on totally dissolved material) where LOI (Loss on ignition) corresponds mainly to a loss of water or CO_2 at high temperature and C_{org} corresponds to organic carbon measured by C/S analyser

	SiO_2	Al_2O_3	Fe_2O_3	MnO	MgO	CaO	Na_2O	K_2O	TiO_2	P_2O_5	LOI	Total	C_{org}
Intact	48.8	17.1	6.7	0.034	2.4	7	0.50	1.3	0.9	**0.33**	14.1	99.2	**0.26**
3 cycles	49	18.1	7.2	0.026	2.2	5.1	0.64	1.2	0.9	**0.31**	13.9	98.7	**0.57**
6 cycles	45.1	16.7	6.6	0.037	2.3	8.4	0.66	1.2	0.85	**0.32**	16.7	99.0	**0.73**

adsorption on clay surface and the low content of P or S limited the quantity of precipitated phases. However, the presence of theses pollutants in pore water impacted the ionic force and changed the electrical double layer width. The soil particles tended to be more aggregated/flocculated with lower particle dispersion. Such process may induce a fissuring inter or intra-aggregates which should contribute to the loss of soil cohesion as observed during the direct shear test and the degradability test.

Finally, a slight increase of the organic carbon content C_{org} from 0.26 to 0.73 was observed after wet/dry cycles in contact with polluted water in Table 4. Even if the concentration of laundry detergents was fixed to a high amount (close to 60 g/L), the organic compound uptake by compact marly soil specimen remained low considering the limited quantity of pore water that allowed the pollutant diffusion until a soil surface site of adsorption. Among compounds met in laundry detergents, anionic surfactants used as washing agents were present but even then, their negative charge probably contributed to lower their effect on soil, especially on clays (Amirianshoja et al. 2013). However, their presence in pore water even at low content changed the surface tension, lowering the contact angle (which impacts the capillary phenomenon—Akbulut et al. 2012) and then impacting the pore suction and the force of interaction between particles.

3.3 Effects of Wet/Dry Cycles on Marly Soil Fragmentation

The grain size of crushed soil used for the standardized degradability test was measured before and after the application of 4 wet/dry cycles. The structural evolution of marly soil can be observed by eye on Fig. 7. Before testing, the sample was mainly composed of large elements but after four wet/dry cycles, the fine content increased. The soil degradation consisted in a decrease of the blocks diameter, and the polluted water showed a stronger effect, compared to distilled water.

To be more quantitative, the Fig. 8 shows the particle size distributions of the marly soil obtained before and after the degradability test. The degradation induced smaller blocks of soil with the appearance of a 20 and 40% fraction less than 5 mm in contact with unpolluted water and polluted water respectively. Results confirmed that the degradation was greater in presence of polluted water, as expected with an increase of ionic force (in polluted water) that promoted the soil flocculation/aggregation and its micro fissuring. Pollutants accelerated the soil degradation but water by itself was enough to strongly damage the structure of marly soil.

The soil degradation was also observed at microscale by using SEM completed by porosity measurements. The Fig. 9 shows the microstructure of intact soil that was mainly layered in one place (Fig. 9a and b) and more compact and uniform in another place (Fig. 9c and d). Layers presented some flat surfaces with low rugosity (secondary phases such as quartz and carbonates were embedded in clay matrix). Clearly, the presence of such flat surfaces oriented towards the natural sedimentation plan favoured the soil disaggregation into piece of sheet.

After 6 wet/dry cycles in polluted water, the sample was totally disintegrated at macroscale (higher than the millimeter scale). At microscale (at micrometer scale), its structure was similar to that of intact carbonated clay-rich soil. It seems that the degradation process concerned only macroscale. However, the plane surface seemed to be rougher (Fig. 10a and b) as the particles/aggregates were more dispersed with a lower cohesion. The clay matrix had a lower action as cement between secondary phases such as quartz or carbonates, whose sizes were around 5–10 µm diameter. No coarse particles (except aggregates of small particles) were detected and gypsum on Fig. 10c was observed rarely and locally as well as small clustered pyrite particles in light grey on Fig. 10d.

3.4 Effect of Wet/Dry Cycles on Marly Soil Porosity

The soil porosity was measured on samples before and after wet/dry cycles either in distilled water or in polluted water. The Fig. 11 shows the evolution of the soil porosity explored by mercury intrusion porosimetry until 6/10 nm. As observed at microscopic scale with the degradability test. Figure 11 shows some changes on pore size distribution of marly soil. Intact sample presented a monomodal distribution of pore dimensions. Only nanopores between 6 and 100 nm (centred around 20–25 nm) existed in intact soil. After wet/dry cycles, a bimodal behaviour was

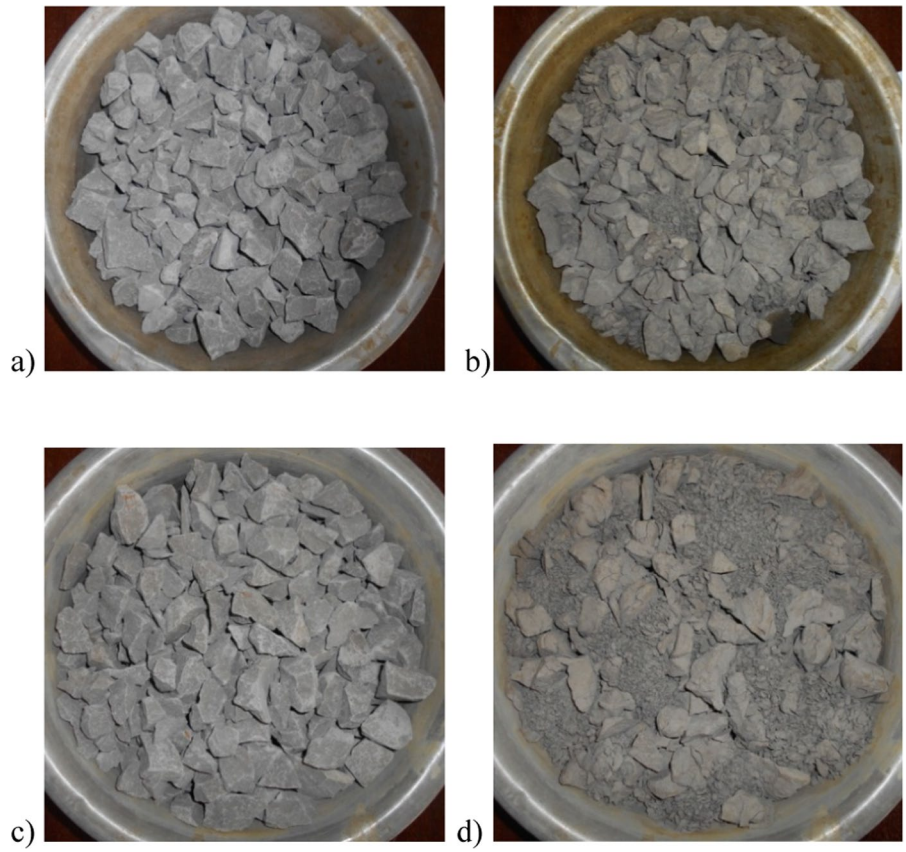

Fig. 7 Degradation of marly soil before and after four wet-dry cycles. **a** and **c** initial state, **b** state after wet/dry cycles with unpolluted water, **c** state after wet/dry cycles with (LC) polluted water

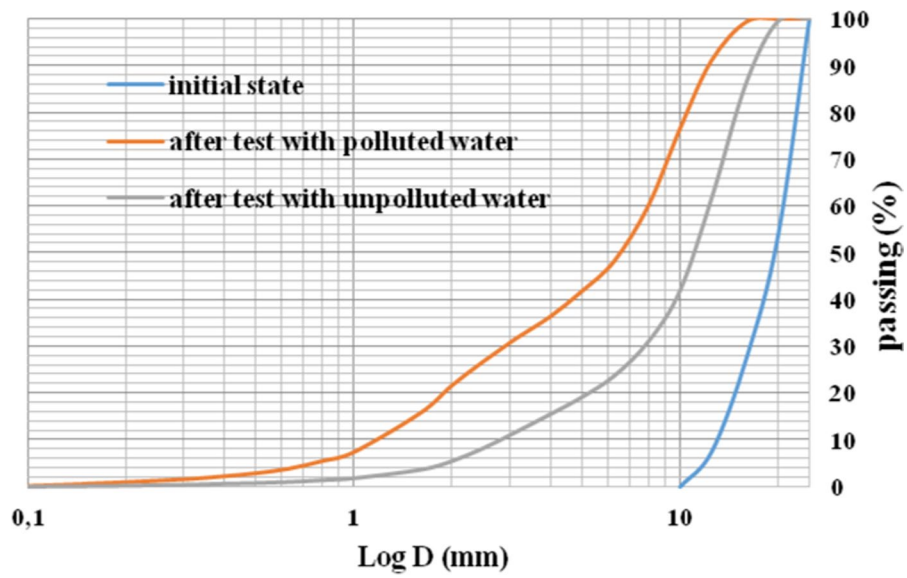

Fig. 8 Particles size distribution curves on carbonated clay-rich soil before and after wet/dry cycles **with** unpolluted or (LC) polluted water

observed on all samples after cycles in polluted or unpolluted water. Macropores (that could correspond to fissuring between blocks observed by SEM on Figs. 9 and 10) appeared with a diameter around 30 µm after contact with polluted and unpolluted water, respectively.

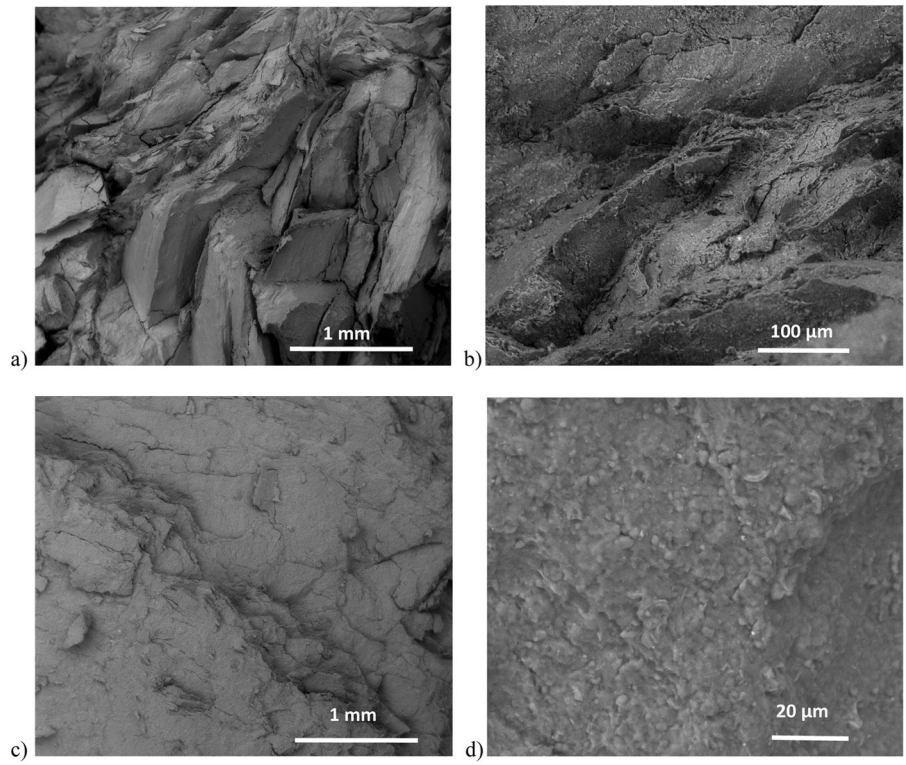

Fig. 9 SEM images of fresh fractured surface of intact marly soil (image in backscattered electron mode) showing **a** at low and **b** at high magnification compact elongated aggregates oriented towards the flat betting of soil and with clear borders (plan of potential disaggregation). Observation **c** at low magnification and **d** at higher magnification of compact surface composed by stacked clay-rich layers

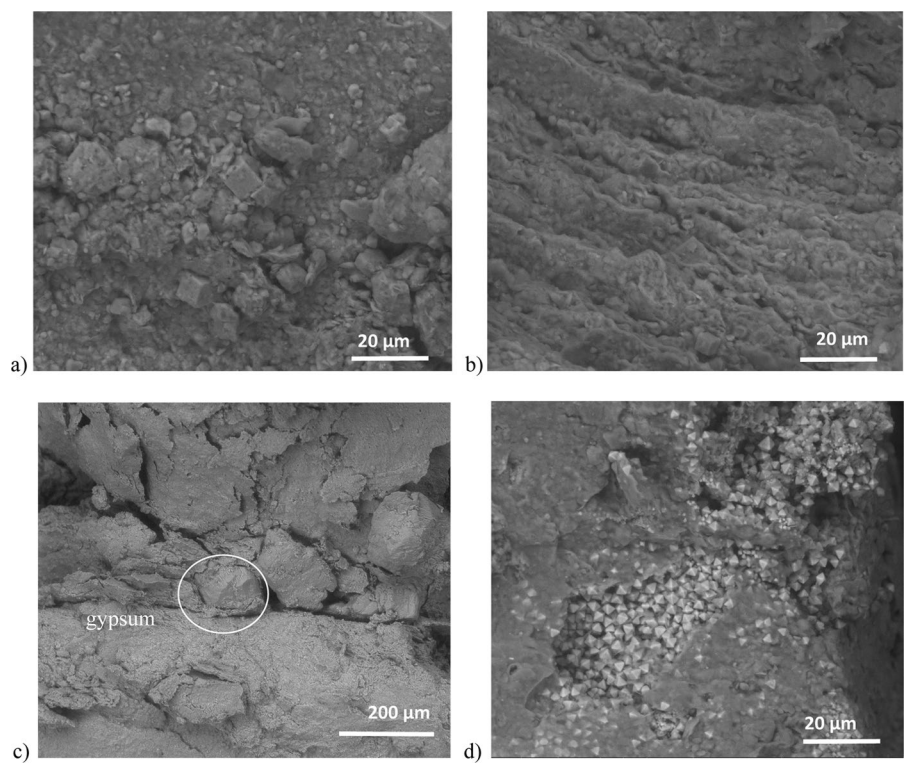

Fig. 10 SEM observations of carbonated clay-rich soil after 6 cycles with (LC) polluted water (image with backscattered electrons mode). **a** and **b** Fresh fractured rough surface with a higher particle aggregation, **c** Local observation of isolated gypsum grain in disaggregated space and **d** local cluster of pyramidal pyrite particles in light grey

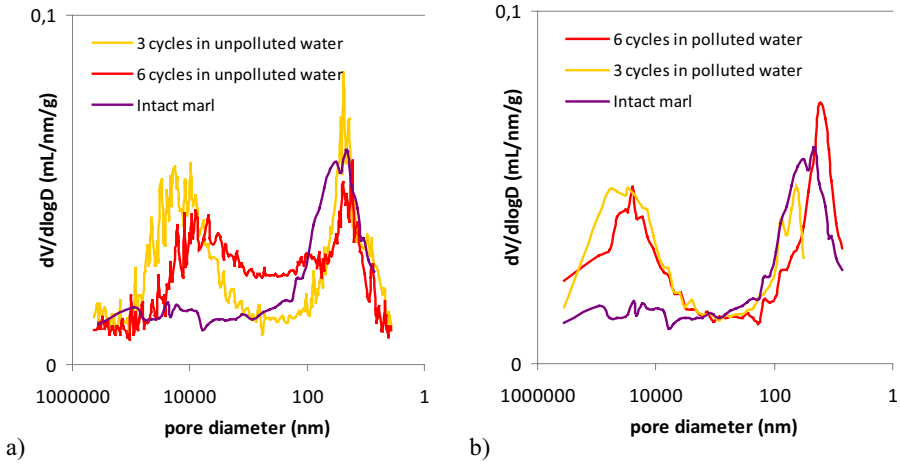

Fig. 11 Pore size distribution obtained by porosimetry by mercury intrusion in marly soil versus the number of applied wet/dry cycles: **a** with unpolluted water, **b** with (LC) polluted water

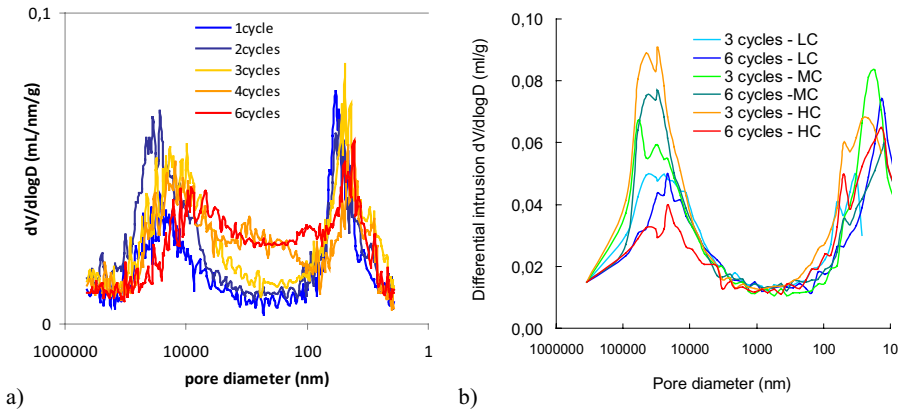

Fig. 12 Pore size distribution obtained by mercury intrusion porosimetry in marly soil versus the number of applied wet/dry cycles: **a** with unpolluted water, **b** with low concentrated (LC) polluted water, with medium concentrated (MC) polluted water and highly concentrated (HC) polluted water

The effect at microscale on the pore size distribution seemed to be similar whatever the characteristics of water. However, in unpolluted water some additional pores between macro and nanopores occurred after 6 cycles compared to the distribution collected after three cycles. Such new pore population could be due to the thinning process of some initial macropores after reorganisation/compaction during the drying steps. Such hypothesis was reinforced by the following of the pore size distribution step by step after 1 to 6 cycles on Fig. 12a. Such effect was not observed with polluted water and was confirmed by the collect of the pore size distribution on carbonated clay-rich soil put in contact with polluted water at medium and high concentration of pollutants on Fig. 12b. The higher the pollutant concentration was, the more numerous the macropores were after a few cycles. Indeed, the increase of the number of applied cycles seemed to decrease the macropores population after 6 cycles because of soil particles reorganization (compaction effect of the drying step). Such behaviour was also observed on the cumulative mercury intrusion curves from which the total soil porosity in Table 5 was determined.

Table 5 The soil porosity measured by mercury intrusion porosimetry versus the number of applied cycles with polluted or unpolluted water (MC: medium concentrated polluted water and HC: highly concentrated polluted water)

Sample	Porosity (%) (with unpolluted water)	Porosity (%) (with polluted water)
Intact soil	19.2	
1 cycle	19.2	–
2 cycles	23.7	–
3 cycles	26.9	25.1 (22.3 MC) (26.9HC)
4 cycles	26.9	–
6 cycles	25.3	25.2 (18.9MC) (22.7HC)

The volume of injected mercury increased with first cycles (that caused the soil disaggregation). The initial porosity on intact carbonated clay-rich soil was estimated close to 19.2% by MIP while the porosity n evaluated by geotechnical way was estimated to 30%. Such difference could be due to the soil heterogeneity but also to the size of the tested sample (less than 1 cm^3 for mercury intrusion porosimetry and 70–100 cm^3 for geotechnical test) or more probably, to the fact that mercury could not explore all the porosimetry below 10 nm. After the initial increase of the total porosity, a decrease of the porosity was observed in Table 5 after 6 wet/dry cycles in both polluted or unpolluted waters.

3.5 Effect of Wet–Dry Cycles on Mechanical Properties

The direct shear tests (in drained consolidated conditions) allowed to evaluate the strength characteristics of marly soil (via the friction angle φ' and the cohesion c') after an increasing number of wet–dry cycles before test. The Fig. 13 shows the shear strain versus the shear stress curves before and after water degradation by immersion, for a normal stress of 400 kPa. The curves from direct shear test did not show a rupture peak, but in most case, a plateau appeared from a particular displacement. The observed shapes of the curves were similar for normal stresses of 100 kPa and 300 kPa. The maximum stresses measured on intact marly soil, corresponded to a ductile deformation rather than a brittle failure. This behaviour agreed with tests conducted on remoulded soil specimens that behaved as recent geological clay-rich formation.

The synthesis of the tests carried out is presented in Fig. 14, which shows that the most impacted parameter is the cohesion.

Based on Mohr-Coulomb criterion, the direct shear test allowed to evaluate the values of cohesion c' and friction angle φ' reported in Table 6. The intact marly soil presented a cohesion equal to 49.9 kPa combined with an average friction angle around 20.8°. Concerning the soil samples subjected to wet/dry cycles with polluted or unpolluted water, the cohesion measured after cycles decreased with the number of cycles both with polluted or unpolluted water, while the friction angle kept almost the same value around 20°. The cohesion decreased from 49.9 to 45.5 kPa with distilled water while the polluted water induced a higher decrease until 31.5 kPa. Therefore, the effect of pollutants in water clearly diminished the cohesion. Such result agreed with the results of the degradability test, the results of MIP and SEM observation: indeed, Figs. 11 and 12 show the appearance after a few wet/dry cycles of macropores that can be associated with the disaggregation of the matrix, and can therefore lead to a decrease of the cohesion. Furthermore, Fig. 10c, achieved through SEM observation clearly shows the same phenomena, with a clear apparition of cracks in the matrix that can be directly linked to a decrease of the soil cohesion. In presence of pollutants as met in wastewater, an increasing number

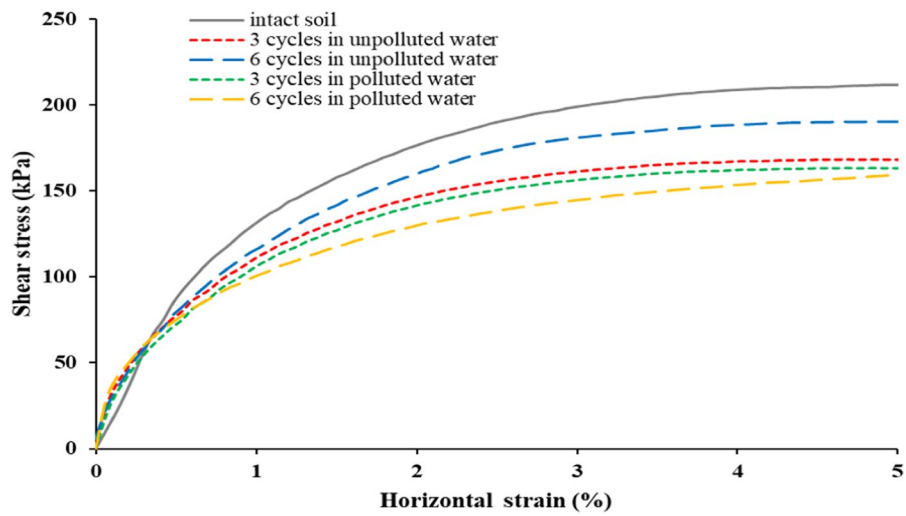

Fig. 13 Horizontal stress versus horizontal strain obtained during direct shear test before and after degradation under (LC) polluted water effect (test for a normal stress of 400 kPa)

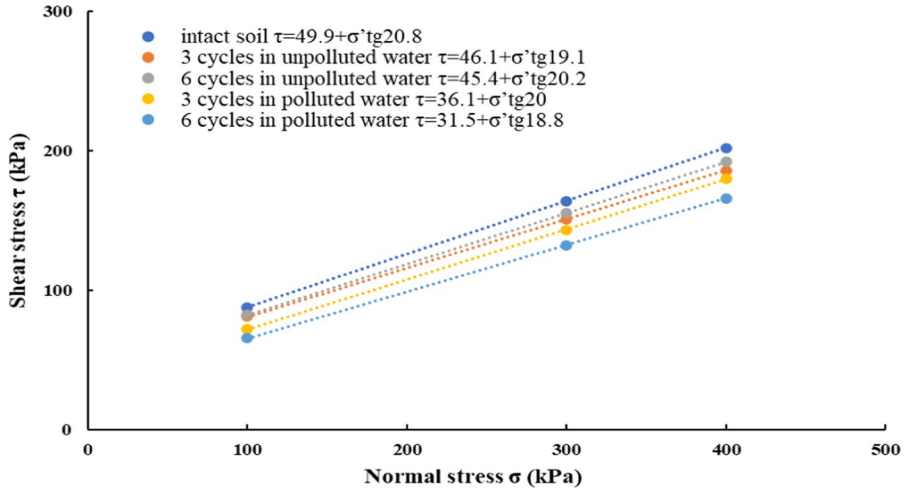

Fig. 14 Evolution of the failure envelope of the soil linked to the numbers of applied cycles with unpolluted water or (LC) polluted water

Table 6 Cohesion and friction angle from shear stress test of marly soil according to the number of cycles and the nature of water

Sample	Cohesion c' (kPa)	Friction angle φ' (°)
Intact soil	49.9	20.8
Soil after 3 cycles in unpolluted water	46.1	19.1
Soil after 6 cycles in unpolluted water	45.4	20.2
Soil after 3 cycles in polluted water	36.1	20.0
Soil after 6 cycles in polluted water	31.5	18.8

of cycles favoured the ability of soil samples to be crushed.

4 Conclusion

This study produced a multi-scale characterization before and after wet/dry cycles applied on a compact marly soil from Azazga landslide area. Results confirmed that the water circulation in ground remains the preponderant cause to explain the landslide reactivation. In Azazga landslide area, the infiltration and percolation of polluted or unpolluted water along fractures probably act as a lubricant to promote the initiation or reactivation of landslide and such effect was enhanced by a specific soil degradation under wet/dry cycles combined with the presence of pollutants in water.

As demonstrated by tests in this study, water without chemical content (such as pollutants) was able to degrade the material mainly by disaggregation or fragmentation into blocks rather than by particles dispersion. The degradability tests at macroscale (at millimeter scale) showed after wet/dry cycles the appearance of a < 5 mm fraction and the diminution of the diameter of soil blocks. Such disaggregating effect caused by water and enhanced by pollutants was confirmed at microscale by SEM observations and by mercury intrusion porosimetry measurements. A microstructure composed by oriented plans or grains with plane surfaces favoured the soil disaggregation by offering some preferential route to water. The appearance of macropores after only one wet/dry cycle (with or without pollutants in water) agreed with such description. The water pollution led to changes in the microstructure and showed an increase in porosity from 19 to 25% depending on the number of drying-wetting cycles.

Contributing to the soil microstructure, water has also an effect on the soil mechanical characteristics by reducing the shear resistance. Indeed, if the friction angle of tested soil remained quite stable even after degradation at about 20°, the cohesion decreased from 49.9 to 31.5 kPa with the number of wet/dry cycles especially in presence of pollutants in water.

In comparison, the soil mineralogy (with around 30.6% of quartz, 12.5% of carbonates and 45.1% of clays) was only slightly impacted by the presence of pollutants even if the polluted water contained 20 mg/L of phosphates, 40 mg/L of sulphates and

60 g/L of laundry detergents. No new phases were observed by XRD except gypsum precipitation. Few carbonates dissolved as well as amorphous silica, which explained the increase of the Si content after degradation. Furthermore, the cations composition in montmorillonite interlayer probably changed after contact with polluted water and a Ca increase could explain the shift of the d spacing related to the crystalline clay swelling and its ability to adsorb water during immersion or to shrink during the drying. In addition, the presence of pollutants in pore water acted actively on the electrical double layer width (effect of ionic species) and/or on the wettability of the pore surface (surfactant effect). Therefore, they played probably a major role on the change of microstructure conducting to an enhanced fragmentation in contact with polluted water.

References

AFNOR NF P 94-067 (1992) Degradability coefficient of rocky material. French standard

AFNOR NF P 94-051 (1993) Determination of Atterberg's limits, Liquid limit test using Casagrande apparatus, plastic limit test on rolled thread. French standard

Akbulut S, Kurt ZN, Arasan S (2012) Surfactant modified clays' consistency limits and contact angles. Earth Sci Res J 16(2):95–101

Ameur N (2014) Analyse et évaluation du potentiel de risque du glissement de terrain d'Azazga. master thesis. University of Mouloud Mammeri Tizi-ouzou, Algeria

Amirianshoja T, Junin R, Idris AK, Rahmani O (2013) A comparative study of surfactant adsorption by clay minerals. J Petrol Sci Eng 101:21–27. https://doi.org/10.1016/j.petrol.2012.10.002

Aurelie V (2010) Processus et bilans d'altération en milieu tropical (bassin versant de Mule Hole, Inde du Sud): Sensibilité à la composition Minéralogique et au climat. PhD thesis. University of Toulouse III, France

Boukoffa M (2018) Les phénomènes d'altération (superficielles) des roches silicates alumineuses (granitiques et gneissiques) des massifs de petite Kabylie (NE Algérien): conséquences au point de vue minier et hydrogéologique. PhD thesis. University of Annaba, Algeria

Bower H (2002) Artificial recharge of ground water: hydrogeology and engineering. Hydrogeol J 10:121–142. https://doi.org/10.1007/s10040-001-0182-4

Brindley GW (1980) Crystal Structures of Clay Minerals and Their X-Ray Identification, Mineralogical Society Monograph, N°5. Mineralogical Society. ISSN 0144.1485. ISBN 0 903056 08 9, London, pp. 485

Bufalo M, Oliveros C, Quélennec RE (1989) L'érosion des terres noires dans la région du Buëch (Hautes-Alpes). Contribution à l'étude des processus érosifs sur le bassin versant représentatif (BVRE) de Saint-Genis. La Houille Blanche 3-4193-195. https://doi.org/10.1051/lhb/1989012

Burnol A, Duro L, Grive M (2006) Eléments traces métalliques. Guide méthodologique, recommandations pour la modélisation des transferts des éléments traces métalliques dans les sols et les eaux souterraines. Rapport final, N°INERIS-DRC-06-66246/DESP-R01a, 23–54

Cafaro F, Cotecchia F (2001) Structure degradation and changes in the mechanical behavior of a stiff clay due to weathering. Geotech 51:441–453. https://doi.org/10.1680/geot.2001.51.5.441

Campy M, Macaire JJ (2003) Géologie de la surface. Erosion, transfert et stockage dans les environnements continentaux. Quaternaire 14(4):279–280

Chen R, Ng CWW (2013) Impact of wetting-drying cycles on hydro-mechanical behavior of an unsaturated compacted clay. Appl Clay Sci 86:38–46. DOI: https://doi.org/10.1016/j.clay.2013.09.018

Chodzko J, Lecompte M (1992) Ravinement dans les Baronnies. Travaux du laboratoire de géographie physique 20:1–109

Clark M, Small J (1982) Slopes and weathering. Cambridge Topics in Geography. 2ième series. Cambridge University Press, Cambridge, 12 p

Colas G, Dumolard B (1988) Erodabilité des marnes. Rapport interne du centre d'étude technique et de l'équipement méditerranée CETE, Aix-en-Provence. 108 p

Collin ML, Melloul AJ (2003) Assessing groundwater vulnerability to pollution to promote sustainable urban and rural development. J Clean Prod 11(7):727–736. https://doi.org/10.1016/S0959-6526(02)00131-2

Djerbal L, Alimrina N, Melbouci B, Bahar R (2014) Mapping and management of landslide risk in the city of Azazga (Algeria). Landslide science for a Safer Geoenvironment. Springer, Cham, pp 463–468. https://doi.org/10.1007/978-3-319-05050-8_72

Duc M, Makki L, Lamas-Lopez F, Magnan J-P (2014) Impact of the wet-dry cycles on intact or remolded clayey and marly soils. Proceeding of JNGG2014, Beauvais 8–10 July 2014, France

Fifi U, Winiarski T, Emmanuel E (2009) Sorption mechanisms studies of Pb(II), Cd(II) and Cu(II) into Soil of Port-au-Prince. J Int Hydrol Programme Latin Am Caribbean Aqua-LAC 1(2):164–171

Emmanuel S, Anovitz LM, Day-Stirrat RJ (2015) Effects of coupled chemo-mechanical processes on the evolution of pore-size distributions in geological media. Rev Mineral Geochem 80(1):45–60. https://doi.org/10.2138/rmg.2015.03

Gabet EJ, Wolff-Boenisch D, Langner H, Burbank DW, Putkonen J (2010) Geomorphic and climatic controls on chemical weathering in the high Himalayas of Nepal. Geomorphology 122:205–210. https://doi.org/10.1016/j.geomorph.2010.06.016

Gélard JP (1979) Géologie du Nord-Est de la grande Kabylie. Phd thesis. University of Dijon, France

Geremew Z, Audiguier M, Cojean R (2009) Analyse du comportement d'un sol argileux sous sollicitations hydriques cycliques. Bull Eng Geol Environ 68:421–436. DOI: https://doi.org/10.1007/s10064-009-0203-4

Goh SG, Rahardjo H, Leong EC (2014) Shear strength of unsaturated soils under multiple drying-wetting cycles. J Geotech GeoEnviron Eng 140(2):06013001. https://doi.org/10.1061/(ASCE)GT.1943-5606.0001032

Goodfellow BW, Hilley GE, Webb SM, Sklar LS, Moon S, Olson CA (2016) The chemical, mechanical, and hydrological evolution of weathering granitoid. J Geophys Res Earth Surf 121:1410–1435. https://doi.org/10.1002/2016JF003822

Guigo M (1979) Hydrologie et érosion dans l'Apennin septentrional. Thesis of University Aix Marseille II, France

Guilloux A, Cojean R, Doré M (2005) Note sur la définition des « sols Indurés Roches Tendres (SIRT). Revue Française de Géotechnique 111:59–66

Hamès V, Lautridou JP, Oze A, Pissart A (1987) Variations dilatométriques de roches soumises à des cycles « humidification-séchage ». Géographie Phys et Quaternaire 41(3):345–354. https://doi.org/10.7202/032690ar

Hausrath EM, Navarre-Sitchler AK, Sak PB, Williams JZ, Brantley SL (2011) Soil profiles as indicators of mineral weathering rates and organic interactions for a Pennsylvania diabase. Chem Geol 290(3–4):89–100. https://doi.org/10.1016/j.chemgeo.2011.08.014

Hounsounou EO, Agassounon Djikpo Tchipozo M, Kelome NC, Vissin EW, Mensah GA, Agbossou E (2016) Pollution des eaux à usages domestiques dans les milieux urbains défavorisés des pays en développement: synthèse bibliographique. Int J Biol Chem Sci 10(5):2392–2412. https://doi.org/10.4314/ijbcs.v10i5.35

Iniguez Herrero J (1967) Altération des calcaires et des grès utilisés dans la construction. Ed. Eyrolles, Paris

Labus M, Bochen J (2012) Sandstone degradation: an experimental study of accelerated weathering. Environ Earth Sci 67:2027–2042. https://doi.org/10.1007/s12665-012-1642-y

LCTP (2004) Étude géotechnique d'urbanisation POS A1 et A5 azazga. Dossier N° 31.04.0049.

LCTP (2003) Etude géotechnique des POS D1 et D2 de la ville d'Azazga.Dossier N°31.03.0042. 9.

Li J, Zhou K, Liu W, Zhang Y (2018) Analysis of the effect of freeze thaw cycles on the degradation of mechanical parameters and slope stability. Bull Eng Geol Environ 77:573–580. https://doi.org/10.1007/s10064-017-1013-8

Lofi J, Pezard P, Loggia D, Garel E, Gautier S, Merry C, Bondabou K (2012) Geological discontinuities, main flow path and chemical alteration in a marly hill prone to slope instability. Assessment from petrophysical measurements and borehole image analysis. Hydrol Proces 26:2071–2084. https://doi.org/10.1002/hyp.7997

LTPC (1987) Etude géotechnique de la ville d'Azazga. Dossier N° 27:851012

Mamillan M, Bouineau A (1982) Effets de la "pollution climatique" sur la pierre. 4ème symposium sur la recherche en matière de pollution atmosphérique. Arles, 29 p

Medjnoun A, Bahar R (2016) Shrinking–swelling of clay under the effect of hydric cycles. Innov Infrastruct Solut 1:46. DOI:https://doi.org/10.1007/s41062-016-0043-6

Melki S, Mabrouk El Asmi A, Gueddari M (2019) Inferred industrial and agricultural activities impact on groundwater quality of Skhira coastal Phreatic aquifer in southeast of Tunisia (Mediterranean region). Hindawi Geofluids 2019. https://doi.org/10.1155/2019/9465498

Molina Ballesteros E, Cantono Martín M, García Talegón J (2010) Role of porosity in rock weathering process: a theoretical approach. Cad Lab Xeol Laxe 35:147–162

Monnet J, Fabre D, Zielinski M (2012) Freeze-thaw and degradation of marly rock: the black marl example. Journées Nationales de Géotechnique et de Géologie de l'Ingénieur. Bordeaux 4–6 juillet 2012.

Mulliss RM, Revitt DM, Shutes RBE (1997) The impacts of discharges from two combined sewer overflows on the water quality of an urban watercourse. Water Sci Technol 36(8–9):195–199. https://doi.org/10.1016/S0273-1223(97)00599-4

Office National d'Assainissement (ONA) (2016) Note interne, 12 Juin 2016

Office National de Météorologie (ONM) (2016) Note interne

Ogunsola NO, Olaleye BM, Saliu MA (2017) Effects of weathering on some physical and mechanical properties of Ewekoro limestone, south-western Nigeria. Int J Eng Appl Sci 4(11):72–82

Pires LF, Cooper M, Cásaro FAM, Reichardt K, Bacchi OOS, Dias NMP (2008) Micromorphological analysis to caracterize structure modifications of soil samples submitted to wetting and drying cycles. CATENA 72:297–304. https://doi.org/10.1016/j.catena.2007.06.003

Pitt R, Clark S, Field R (1999) Groundwater contamination potential from stormwater infiltration practices. Urban Water 1(3):217–236. https://doi.org/10.1016/S1462-0758(99)00014-X

Pomerol C, Renard M, Lagabrielle Y (2005) Éléments de géologie. Dunod, Paris, p 762

Porokhovoï E (1995) Stabilité à long terme des talus de mines à ciel ouvert dans les massifs de roches basiques et ultrabasiques. PhD thesis. Ecole nationale des ponts et chaussées, France

Quénée B(1990) Transformations minéralogiques et texturales de matériaux rocheux, mortiers et bétons d'ouvrages variés. Approche de la cinétique des mécanismes et identification des facteurs responsables. PhD thesis of University Henri Poincaré in Nancy, France

Saad A, Guedon S, Bost M, Mertz JD, Martineau F (2010) Comparaison en laboratoire de l'altération par gélivation et par dissolution d'une roche calcaire. Journées Nationales de Géotechnique et de Géologie de l'Ingénieur, Grenoble

Serratrice JF (2017) Divers aspects du comportement mécanique des marnes en laboratoire. Rev Fr Geotech 3(151):1–19. https://doi.org/10.1051/geotech/2017007

Sousa LMO, Suárez del Río LM, Calleja L, Ruiz de Argandoña VG, Rodrguez Rey A (2005) Influence of microfractures and porosity on the physico-mechanical properties and weathering of ornamental granites. Eng Geol 77:153–168. https://doi.org/10.1016/j.enggeo.2004.10.001

Tindall AJ (1999) Unsaturated zone hydrology for scientist and engineers. Prentice-Hall. Inc., New Jersey, p 624

Tisdall JM, Cockroft B, Uren NC (1978) The stability of soil aggregates as affected by organic materials, microbial activity and physical disruption. Aust J Soil Res 16(1):9–17. https://doi.org/10.1071/SR9780009

Tran TD (2014) Rôle de la microstructure des sols argileux dans les processus de retrait-gonflement: de l'échelle de l'éprouvette à l'échelle de la chambre environnementale. PhD thesis of Graduate School-Mines ParisTech, France

Tripathy S, Subba Rao KS, Fredlund D (2002) Water content void ratio swell-shrink paths of compacted expansive soils. Can Geotech J 39:938–959. https://doi.org/10.1139/t02-022

Tugrul A (2004) The effect of weathering on pore geometry and compressive strength of selected rock types from Turkey. Eng Geol 75:215–227. https://doi.org/10.1016/j.enggeo.2004.05.008

Viville D, Chabaux F, Stille P, Pierret MC, Gangloff S (2012) Erosion and weathering fluxes in granitic basins: the example of the Strengbach catchment (Vosges massif, eastern France). CATENA 92:122–129. https://doi.org/10.1016/j.catena.2011.12.007

Wells T, Binning P, Willgoose G, Hancock G (2006) Laboratory simulation of the salt weathering of schist: 1. Weathering of schist blocks in a seasonally wet tropical environment. Earth Surf Proc and Landf 31:339–354. https://doi.org/10.1002/esp.1248

Zhang W, Keller AA, Yue D, Wang X (2009) Management of urban road runoff containing PAHs: probabilistic modelling and its application in Beijing, China. J Am Water Resour Assoc 45(4):1009–1018. https://doi.org/10.1111/j.1752-1688.2009.00343.x